JOURNAL OF VIROLOGY, Oct. 2007, p. 10636–10648 Vol. 81, No. 19
0022-538X/07/$08.00+0 doi:10.1128/JVI.01119-07

Incorporation of Functional HN-F Glycoprotein-Containing Complexes into Newcastle Disease Virus Is Dependent on Cholesterol and Membrane Lipid Raft Integrity▽

Jason P. Laliberte,[1] Lori W. McGinnes,[2] and Trudy G. Morrison[1,2]*

Program in Immunology and Virology[1] and Department of Molecular Genetics and Microbiology,[2] University of Massachusetts Medical School, 55 Lake Avenue North, Worcester, Massachusetts 01655

Received 23 May 2007/Accepted 5 July 2007

Newcastle disease virus assembles in plasma membrane domains with properties of membrane lipid rafts, and disruption of these domains by cholesterol extraction with methyl-β-cyclodextrin resulted in the release of virions with irregular protein composition, abnormal particle density, and reduced infectivity (J. P. Laliberte, L. W. McGinnes, M. E. Peeples, and T. G. Morrison, J. Virol. 80:10652–10662, 2006). In the present study, these results were confirmed using Niemann-Pick syndrome type C cells, which are deficient in normal membrane rafts due to mutations affecting cholesterol transport. Furthermore, cholesterol extraction of infected cells resulted in the release of virions that attached to target cells at normal levels but were defective in virus-cell membrane fusion. The reduced fusion capacity of particles released from cholesterol-extracted cells correlated with significant loss of HN-F glycoprotein-containing complexes detected in the virion envelopes of these particles and with detection of cell-associated HN-F protein-containing complexes in extracts of cholesterol-extracted cells. Extraction of cholesterol from purified virions had no effect on virus-cell attachment, virus-cell fusion, particle infectivity, or the levels of glycoprotein-containing complexes. Taken together, these results suggest that cholesterol and membrane rafts are required for the formation or maintenance of HN-F glycoprotein-containing complexes in cells but not the stability of preformed glycoprotein complexes once assembled into virions.

Membrane architecture and lipid organization are important for many cellular and molecular processes, including protein trafficking, signal transduction, and immunological synapse formation (41). In recent years, the roles of cholesterol and sphingolipids in forming distinct membrane microdomains, termed membrane lipid rafts, have become recognized as important in these processes. The inclusion or concentration of specific molecules in these domains and the exclusion of others likely increases the specificity and efficiency of molecular events occurring at membrane surfaces (40).

The participation of membrane lipid raft domains in the assembly and release of many different enveloped RNA viruses, including retroviruses, filoviruses, orthomyxoviruses, and paramyxoviruses, is well-documented (30). Evidence for lipid raft involvement in virus assembly includes the presence of lipid raft-associated molecules in purified virions, colocalization of viral structural proteins with lipid raft markers, and the biochemical association of viral proteins with lipid raft membranes as defined by detergent-resistant membranes (DRMs) (30, 43). Furthermore, extraction of cholesterol from cellular plasma membranes using methyl-β-cyclodextrin (mβCD) resulted in altered release of several different viruses (33), including human immunodeficiency virus. However, the biological significance of these observations has not been resolved.

Newcastle disease virus (NDV), an avian paramyxovirus (19, 45), also assembles in membrane lipid raft domains (18). Evidence for this conclusion was, first, that lipid raft protein markers caveolin-1 and flotillin-2 were found in purified NDV virions, while a non-lipid raft marker, transferrin receptor, was absent. Second, three of the four main structural components of NDV, the nucleocapsid (NP), hemagglutinin-neuraminidase (HN), and fusion (F) proteins, fractionated with detergent-resistant membranes. Third, a kinetic analysis of DRM association and virion incorporation of each of the viral proteins strongly suggested that assembly occurred in lipid raft domains. The importance of these domains in NDV assembly was suggested by the observation that extraction of plasma membrane cholesterol with mβCD (15, 37, 40) stimulated the release of structurally abnormal particles with reduced infectivity (18). Reduced particle infectivity could not be attributed to the lower levels of cholesterol in virus envelopes, since direct cholesterol depletion of purified virion membranes had no significant effect on infectivity (18). Together with previous results in other virus systems, these results implied that proper assembly was dependent on cholesterol in the assembly membrane. However, the known side effects of mβCD, most notably the rearrangement of the cortical membrane cytoskeleton (17), could not be excluded as the primary cause of the effects of mβCD on the assembly and release of infectious virus.

These studies were extended in order to clarify the functional role of cholesterol in NDV assembly. First, characterization of virus released from Niemann-Pick syndrome type C (NPC) fibroblasts, which are deficient in functional membrane lipid rafts, showed that cholesterol depletion without affecting

* Corresponding author. Mailing address: Department of Molecular Genetics and Microbiology, Room S5-250, University of Massachusetts Medical School, 55 Lake Avenue North, Worcester, MA 01655. Phone: (508) 856-6592. Fax: (508) 856-5920. E-mail: trudy.morrison@umassmed.edu.

▽ Published ahead of print on 25 July 2007.

the cytoskeleton resulted in abnormal NDV release. Cholesterol depletion of infected-cell membranes resulted in the release of virions with normal virus-cell attachment activity but significantly reduced virus-cell fusion activity. These results correlated with loss of detection of HN-F glycoprotein complexes in infected cells and with reduced detection of glycoprotein-containing complexes in virions released from cholesterol-depleted cells. However, direct extraction of cholesterol from the virion envelope had no effect on the detection of HN-F protein-containing complexes or virion attachment and fusion activities. Taken together, the results show that intact lipid raft domains in assembly membranes of infected cells facilitate the proper viral glycoprotein interactions necessary for the generation of a functional and infectious virus particle.

MATERIALS AND METHODS

Cells, virus, and reagents. Normal human embryonic lung (HEL) fibroblasts (a kind gift from Timothy Kowalik, University of Massachusetts Medical School) and Niemann-Pick syndrome type C human fibroblasts (NIH Coriell Cell Repository GM03123) were maintained in Dulbecco's modified Eagle medium (DMEM) supplemented with penicillin-streptomycin, L-glutamine, vitamins, nonessential amino acids, and 10% fetal calf serum (FCS). East Lansing Line (ELL-0) avian fibroblasts from American Type Culture Collection were maintained in DMEM supplemented with penicillin-streptomycin and 10% FCS. NDV strain AV (under biosafety level 3 conditions) and NDV strain B1 stocks were prepared by growth in eggs by standard protocols (26). Methyl-β-cyclodextrin (Sigma-Aldrich) was resuspended in DMEM. Lovastatin (Sigma-Aldrich) was prepared in H_2O and activated as described previously (8). Triton X-100 was purchased from Pierce Biotechnology.

Antibodies. Anti-NDV antibody was raised against UV-inactivated NDV virions (27). Anti-M protein antibody was a monoclonal antibody obtained from Mark Peeples (Ohio State University) (7). HN protein-specific antibodies were anti-A (24), anti-AS (25), and anti-H (38). F protein-specific antibodies were anti-HR1 (23), anti-HR2 (6), anti-F_{tail} (45), anti-F_2-96 (an antipeptide antibody raised against amino acids 76 to 96) (24) and anti-Fu1a (29).

Infections and radioactive labeling. HEL and NPC cells seeded at approximately 3.0×10^4 cells per 35-mm plate and ELL-0 cells seeded at approximately 6.0×10^5 cells per 35-mm plate were grown overnight and then infected with NDV at a multiplicity of infection of 10 in 0.25 ml of medium (under biosafety level 3 conditions for strain AV). After 45 min, 1 ml of medium was added, and monolayers were incubated for 5 to 8 h. For radioactive labeling, cells were radiolabeled at 6 h postinfection for 1 h at 37°C in DMEM supplemented with 50 μCi of [^{35}S]methionine and cysteine per ml (New England Nuclear). At the end of the labeling period, cells were incubated with chase medium (DMEM supplemented with 0.1 mM cold methionine without FCS) for the indicated lengths of time.

Virus purification. Culture supernatants were clarified by centrifugation at 5,000 rpm for 5 min, and then particles in the supernatant were sedimented through 20% sucrose (wt/vol) to a 20 to 65% sucrose interface (24,000 rpm for 10 to 12 h at 4°C using a Beckman SW50.1 rotor). For virion flotation, purified virus taken from 20 to 65% sucrose interface fractions was adjusted to ~60% sucrose (wt/vol) and overlaid on top of ~80% (1.24-g/cm^3) sucrose. The sucrose layer-containing virus was then overlaid with 1 ml of 50% sucrose, 1 ml of 38% sucrose, and 0.5 ml of 10% sucrose in a SW50.1 tube. Samples were subjected to centrifugation at 100,000 × *g* for 18 h at 4°C.

Polyacrylamide gel electrophoresis and Western analysis. To prepare cell extracts, cell monolayers were washed in cold phosphate-buffered saline (PBS) and lysed in TNE buffer (25 mM Tris-HCl, pH 7.4, 150 mM $NaCl_2$, and 5 mM EDTA) containing 1% Triton X-100 and 2.5 mg/ml of *N*-ethylmaleimide. Proteins were resolved on 8% polyacrylamide gels by sodium dodecyl sulfate-polyacrylamide gel electrophoresis (SDS-PAGE) as previously described (18). Proteins were detected by Western analysis as previously described (18). Radioactively labeled proteins were detected by autoradiography as previously described (18). Signals in autoradiographs were quantified using a Fluor-S phosphorimager (Bio-Rad).

Isolation of DRMs. Cell monolayers were washed once in ice-cold PBS, and cells were lysed in ice-cold TNE buffer containing 1% Triton X-100 and 2.5 mg/ml *N*-ethylmaleimide. Lysates were incubated on ice at 4°C for 30 min, and DRMs in extracts were isolated by flotation in sucrose gradients as previously described (18). Gradient fractions were collected from the bottom of the gradient (each fraction was 0.25 ml except for the second fraction, which had a volume of 1 ml). Proteins in each fraction were resolved by 8% SDS-PAGE and detected by Western analysis with the appropriate primary and secondary antibodies. After centrifugation, the densities of all sucrose fractions were measured using a refractometer.

Extraction of cholesterol. ELL-0 cells seeded on 35-mm plates were infected and radiolabeled for 1 h as described above. At the end of the labeling period, monolayers were incubated with chase medium (DMEM supplemented with 0.1 mM cold methionine only) for 1 h. Cells were then either left untreated or treated with 10 mM mβCD and 4 μg/ml lovastatin for 1 h in DMEM supplemented with 0.1 mM cold methionine at 37°C. The medium was then removed and replaced with complete DMEM containing lovastatin, and cells were further incubated for 1 h (immunoprecipitation experiments) or 4 h (virion experiments). Excluding the experiments depicted in Fig. 8, at no time were virus particles incubated in the presence of mβCD.

For the experiments shown in Fig. 8, extraction of cholesterol from NDV particles was performed as described previously (18). Briefly, nonradiolabeled or ^{35}S-radiolabeled, gradient-purified NDV (strain AV) virions from untreated ELL-0 cells were mixed with DMEM or with increasing concentrations of mβCD in DMEM and incubated for 1 h at 37°C. The virus was purified away from mβCD-cholesterol complexes by sedimentation through 20% sucrose as described above.

Immunofluorescence of surface HN and F glycoproteins. HEL, NPC, and ELL-0 cells were grown to confluence on glass coverslips in 35-mm plates and infected with NDV (strain AV) for 7 h. Cells were then left untreated or treated with 10 mM mβCD and 4 μg/ml lovastatin for 1 h, followed by a 1-h recovery in DMEM in the presence of lovastatin. Cells were then washed twice with ice-cold immunofluorescence buffer (IF buffer) (PBS containing 1% bovine serum albumin, 0.02% sodium azide, and 5 mM $CaCl_2$), fixed with 2% paraformaldehyde for 10 min on ice, and blocked with IF buffer overnight at 4°C. Cells were then incubated for 1 h at 4°C in IF buffer containing HN protein-specific rabbit anti-H antibody or F protein-specific mouse anti-Fu1a antibody. Following three washes with ice-cold IF buffer, cells were incubated for 1 h at 4°C in IF buffer containing Alexa Fluor 488-conjugated goat anti-rabbit antibody (Molecular Probes) or Alexa Fluor 568-conjugated goat anti-mouse antibody (Molecular Probes). Monolayers were then washed three times with ice-cold IF buffer and incubated for 20 min on ice with IF buffer containing Hoechst nucleus stain (Molecular Probes). Cells were washed twice with ice-cold IF buffer and mounted on slides using Vectashield mounting medium (Vector Laboratories) for fluorescence microscopy. Fluorescence images were acquired using a Nikon fluorescence microscope and Openlab software.

Coimmunoprecipitation of viral proteins. Coimmunoprecipitation was done by the method of McGinnes and Morrison (24). Briefly, equivalent volumes of cellular extracts were incubated overnight at 4°C with a cocktail of HN protein-specific antibodies (anti-A, anti-AS, and anti-H) or a cocktail or F protein-specific antibodies (anti-HR1, anti-HR2, anti-Fu1a, anti-F_{tail}, and anti-F_2-96) or in the absence of antibody. Antibody complexes were precipitated with Pansorbin cells, washed three times in TNE buffer containing 0.5% Triton X-100, and prepared for SDS-PAGE as described above. For DRM gradient fractions, equivalent volumes of sucrose fractions were adjusted to 1% Triton X-100 and incubated overnight at 4°C with the cocktail of HN protein-specific antibodies or F protein-specific antibodies or in the absence of antibody. Antibody complexes were precipitated with Pansorbin cells, washed three times in TNE buffer containing 0.5% Triton X-100, and prepared for SDS-PAGE. The amount of each protein precipitated in the no-antibody sample, due to protein aggregation or nonspecific association of the proteins with Pansorbin cells, was subtracted from the amount of glycoprotein specifically precipitated when NDV-specific antibody was present.

Sorting of virions. ^{35}S-radiolabeled virus (strain AV) was purified by sedimentation through 20% sucrose and subsequently floated as described above. Equivalent amounts of intact virions with normal particle density (1.18 to 1.20 g/cm^3) (18) were incubated overnight at 4°C with either polyclonal anti-NDV antibody, HN protein-specific anti-H antibody, or a cocktail of F protein-specific antibodies (anti-HR1, anti-HR2, anti-F_2-96, and anti-Fu1a) or in the absence of antibody. Antibody-virus complexes were precipitated with Pansorbin cells and washed with cold TNE buffer. The precipitated virions were then adjusted to 1% Triton X-100 to lyse virions. All viral proteins were then immunoprecipitated with a cocktail of NDV-specific antibodies and Pansorbin cells. Precipitates were washed three times in PBS containing 0.4% SDS, and proteins were prepared for SDS-PAGE as described above. To calculate sorting efficiency, background (no-antibody controls) values were subtracted, and then background-adjusted values were divided by the total amount precipitated with anti-NDV antibody.

Virus-cell binding. ^{35}S-radiolabeled, gradient-purified NDV (strain AV) virus from untreated or mβCD-treated ELL-0 cells was incubated with chilled, confluent ELL-0 cell monolayers for 1 h on ice at 4°C in cold Ca^{2+}-rich DMEM. Monolayers were then washed gently three times with cold PBS, and cell extracts were prepared as outlined above. All viral proteins were immunoprecipitated and prepared for SDS-PAGE as described above. The specificity control consisted of preincubation of an equivalent amount of virions with neutralizing anti-NDV antibody for 30 min at room temperature prior to binding with cell monolayers. To calculate binding efficiency, an equivalent amount of virions was immediately lysed, and all viral proteins were immunoprecipitated for the assay input.

Virus-cell fusion. For visualization of R18 virus-cell fusion by fluorescence microscopy, gradient-purified NDV (strain AV) from untreated ELL-0 cells was incubated with R18 (octadecyl rhodamine B; Molecular Probes) for 1 h at room temperature in the dark. R18-loaded particles were purified away from excess R18 by sedimentation through 20% sucrose as described above. ELL-0 cells, grown to confluence on glass coverslips in 35-mm plates, were incubated with R18-loaded virus for 60 min at 4°C on ice. Unbound virions were removed, and cell monolayers were washed three times with cold PBS. Cells were either immediately fixed with 2% paraformaldehyde after virus binding or shifted to 37°C for further incubation prior to fixation. Nuclei were stained, and fluorescence images were acquired as outlined above. The specificity control consisted of preincubation of an equivalent amount of virions with neutralizing anti-NDV antibody for 30 min at room temperature prior to binding with cell monolayers.

For quantitative R18 virus-cell fusion, gradient-purified NDV (strain B1) from untreated or mβCD-treated avian ELL-0 cells was incubated with acetylated trypsin (Sigma-Aldrich) to cleave virion F proteins for 15 min at 37°C as described by Connolly and Lamb (3). Particles were then incubated with soybean trypsin inhibitor (Sigma-Aldrich) for 15 min at room temperature. Virions were then incubated with R18 for 1 h at room temperature in the dark and repurified as described above. Virions were then incubated with chilled guinea pig erythrocytes (Bio-Link, Inc.) in 24-well plates for 1 h on ice at 4°C in the dark. Upon incubation of plates at 37°C, R18 fluorescence (excitation, 560 nm; emission, 590 nm) from wells containing virus and erythrocytes was read at 10-min intervals with a SpectraMax Gemini XS (Molecular Devices) and SoftMax Pro software (Molecular Devices). At the end of 60 min at 37°C, wells were adjusted to 1% Triton X-100 to obtain maximum R18 fluorescence, and experimental values were normalized as described previously (3, 12, 36).

RESULTS

Assembly of NDV in Niemann-Pick syndrome type C human fibroblasts. We have previously reported that extraction of cholesterol from NDV-infected cell membranes with methyl-β-cyclodextrin resulted in the release of structurally abnormal virus particles with reduced infectivity (18). However, incubation of cells with mβCD also results in alterations of the actin cytoskeleton (17). To determine the importance of plasma membrane cholesterol in assembly of NDV in the absence of mβCD effects on the cytoskeleton, assembly of NDV in NPC cells was characterized. NPC cells are human fibroblasts with mutations in one or two genes, *NPC1* and *NPC2*, which result in defective transport of cholesterol to cell plasma membranes and aberrant membrane lipid raft domains (14). Normal human embryonic lung fibroblasts were used as wild-type counterparts for comparison. In contrast to comparisons of untreated and mβCD-treated avian cells (18), the actin cytoskeleton of NPC cells was similar to that of HEL cells (Fig. 1A). HEL and NPC cells were equally permissive to NDV infection. As shown in Fig. 1B, when comparable numbers of HEL and NPC cells were infected with NDV, similar levels of viral protein expression were observed in cellular extracts at 8 h postinfection.

Plasma membrane cholesterol is primarily associated with liquid-ordered domains or membrane lipid rafts (40). These specialized cell surface domains are thought to be experimentally reflected in detergent-resistant membranes, which may be isolated by flotation into sucrose gradients after lysis of cells with nonionic detergents, usually Triton X-100, at 4°C (40). It has been recently recognized that there are two density classes of DRMs, classical DRMs (termed DRM-L with densities of 1.09 to 1.13 g/cm^3) and heavier (higher-density) DRMs (DRM-H), which associate with cytoskeletal components and display buoyant densities of 1.14 to 1.18 g/cm^3 (30). The partitioning of the viral proteins with these DRMs from HEL and NPC cells is shown in Fig. 1C. In results very similar to those observed using infected avian cells, both classes of DRMs from HEL cells contained the hemagglutinin-neuraminidase glycoprotein and the nucleocapsid protein, while the fusion glycoprotein primarily fractionated with DRM-L domains (Fig. 1C). In contrast, significantly reduced amounts of HN and F proteins as well as NP in infected NPC cell extracts fractionated with DRMs (Fig. 1C). These results are consistent with the abnormal lipid raft domains in NPC cells (22).

The release of virus particles from equivalent numbers of infected HEL and NPC cells is shown in Fig. 1D to F. Based upon amounts of NP in purified virions, particle release from NPC cells was enhanced approximately threefold over particle release from HEL cells (Fig. 1D). However, particles released from NPC cells possessed comparable levels of HN protein and slightly reduced amounts of F protein compared to particles released from HEL cells, suggesting there was less glycoprotein per virion in particles released from NPC cells (Fig. 1D).

A comparison of the infectivity of particles released from equivalent numbers of infected HEL and NPC cells showed that infectivity of NPC cell-derived particles was reduced approximately one log unit (PFU/ml) compared to that of HEL cell-derived particles (Fig. 1E). Upon normalization of the infectivity of particles for their NP content, the infectivity of NPC cell-derived particles was approximately 1.5 log unit (PFU/ml) lower than that of particles generated from HEL cells (Fig. 1F). These results, which are very similar to those obtained with untreated and mβCD-treated avian cells (18), support the conclusion that plasma membrane cholesterol and lipid raft domains have a role in the ordered assembly of infectious NDV particles. The results also suggest that the mβCD-induced actin rearrangement is not likely the primary cause of the abnormal virus release from infected cells treated with mβCD (18).

Functional properties of particles released from mβCD-treated cells. To determine the reasons for the decreased infectivity of particles released from mβCD-treated cells (18), attachment of these particles to cells and the fusion of these particles to cell membranes were quantified. The binding activities of ^{35}S-radiolabeled virions, released from untreated or mβCD-treated avian cells, are shown in Fig. 2A and B. Approximately 21% of input particles released from untreated cells bound to target cells, while prior incubation with neutralizing antibody (32) reduced binding to ~1% (Fig. 2B). Similarly, 28% of input particles released from mβCD-treated cells bound to target monolayers, and prior incubation with neutralizing antibody also blocked this binding (Fig. 2B). Thus, cell binding efficiency of particles released from cholesterol-depleted cells was similar to that of normal virions.

The virus-cell membrane fusion activity of these particles was monitored with a R18 fluorescence-based assay, similar to ones described previously (3, 12, 36). The transfer of self-

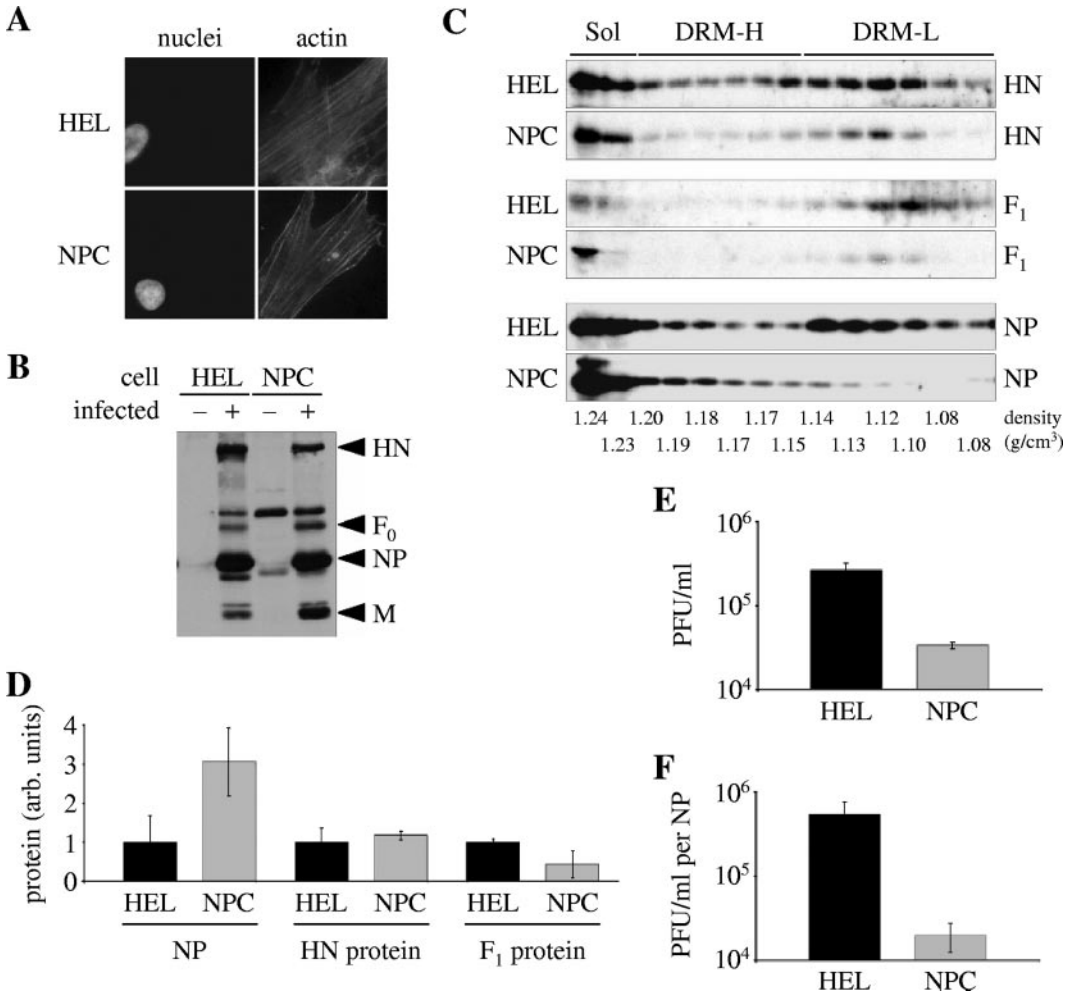

FIG. 1. Abnormal assembly and release of NDV from Niemann-Pick syndrome type C human fibroblasts. (A) Actin distribution of normal human fibroblasts (HEL) and NPC fibroblasts. Uninfected HEL and NPC cells, treated with 0.05% Triton X-100, were incubated with phalloidin (actin panels) for 1 h at 4°C prior to Hoechst staining (panels labeled nuclei). (B) Proteins in uninfected (−) and NDV (B1)-infected (+) HEL and uninfected and NDV (B1)-infected NPC fibroblasts were resolved by SDS-PAGE under nonreducing conditions, and viral proteins were detected by Western analysis with anti-NDV specific antibodies. M, matrix protein; NP, nucleocapsid protein; F_0, uncleaved fusion protein; HN, hemagglutinin-neuraminidase protein. (C) DRMs in extracts of NDV (AV)-infected HEL and NPC cells were isolated by flotation in sucrose gradients as described in Materials and Methods. Proteins present in DRM gradient fractions were detected by Western analysis using anti-NDV (NP), anti-AS (HN protein), or anti-HR2 (F protein). Each lane contains 12% of the corresponding gradient fraction, except for fraction 2, which contains 3% of the total. Densities of each gradient fraction are indicated as g/cm^3. Sol, detergent-soluble gradient fractions; DRM-H, heavy (high-density) DRM gradient fractions; DRM-L, light (low-density) DRM gradient fractions; F_1, cleaved fusion protein. (D) The amounts of NP, HN, and F_1 protein present in purified virions released from equivalent numbers of NDV (AV)-infected HEL and NPC cells detected by Western analysis as described above for panel C. Replicate experiments were quantified by densitometry, and the amount of each protein is represented relative to the amounts detected in virions from HEL cells. (E) Infectivity (PFU/ml), determined by plaque assay as described previously (18, 26), of purified virions released from comparable numbers of NDV (AV)-infected HEL and NPC cells. (F) Infectivity (PFU/ml) normalized for NP protein levels quantified in virions released from comparable numbers of NDV (AV)-infected HEL and NPC cells. Error bars indicate standard deviations.

quenched R18 dimers from viral membranes to that of target erythrocyte membranes involves a hemifusion event, which is mediated by an activated, functional F protein on the viral membrane (28). Fusion is measured by the dequenching of R18 as it spreads into the larger erythrocyte membrane, resulting in increased R18 fluorescence.

The demonstration that this assay can be used to monitor NDV particle fusion with avian cells is shown in Fig. 2C. When virus was bound to cells at 4°C only, no transfer or dequenching of R18 into cell monolayers was observed (Fig. 2C, panel ii). However, incubation of virus-bound cells at 37°C for 30 min or 60 min (Fig. 2C, panel iii or iv, respectively) resulted in transfer and dequenching of R18 into cell monolayers. The transfer of R18 from virions to cells was specific, as preincubation of virus with neutralizing anti-NDV antibody significantly reduced the number of R18-positive cells (Fig. 2C, panel v).

These results were quantified, and the kinetics of virus-cell fusion was determined using a fluorescence plate reader. The hemifusion kinetics of virions released from untreated cells with target cells commenced approximately 10 min following

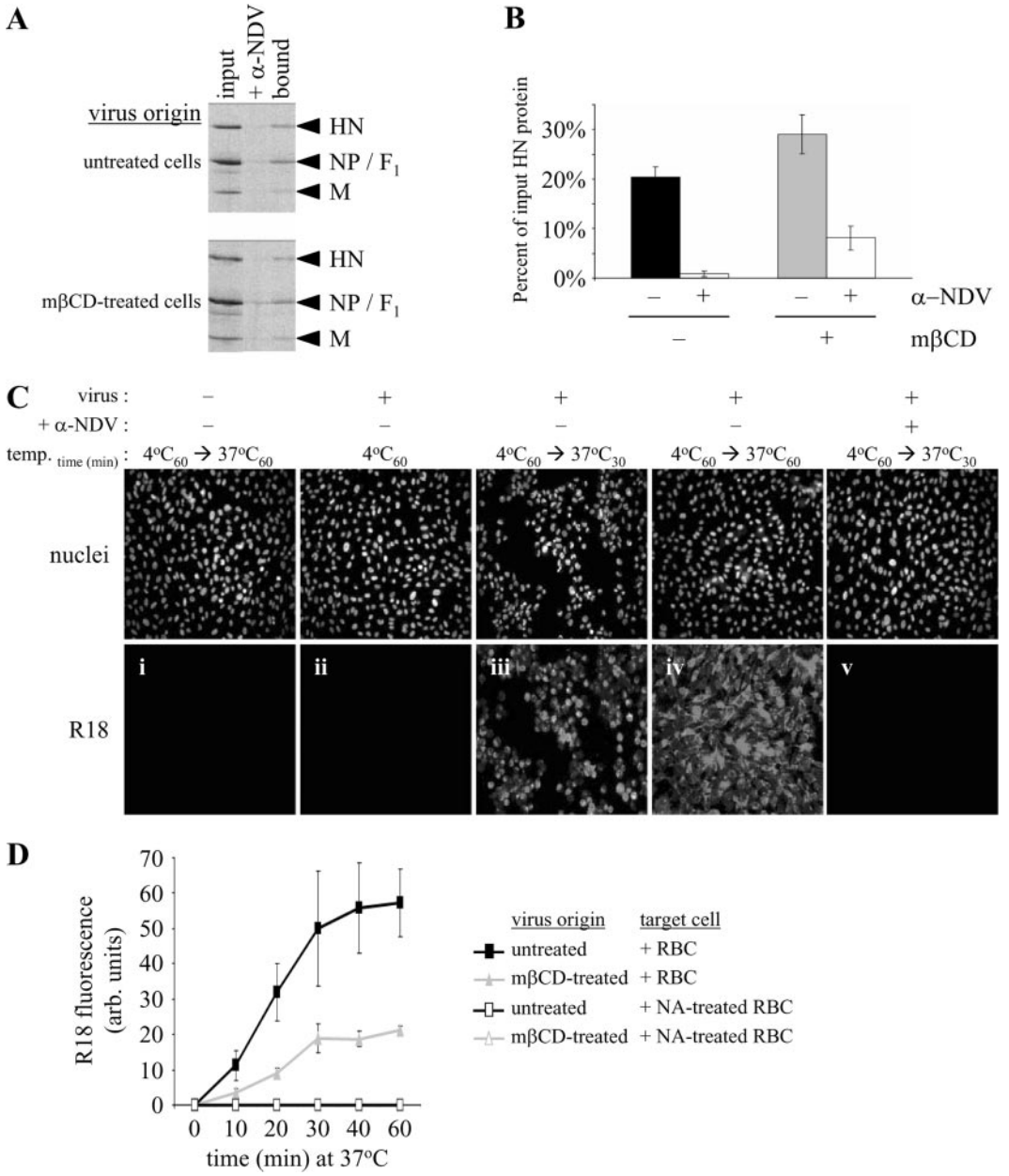

FIG. 2. Attachment and fusion activities of virions released from untreated and mβCD-treated cells. ^{35}S-radiolabeled virions released from untreated or mβCD-treated NDV (AV)-infected ELL-0 cells were purified, and their virus-cell attachment and virus-cell hemifusion activities were characterized as described in Materials and Methods. (A) A representative autoradiograph of cell binding of virions released from untreated and mβCD-treated cells. Virus was bound to avian ELL-0 cells on ice at 4°C for 1 h. Monolayers were washed and lysed, and viral proteins, immunoprecipitated with a cocktail of anti-NDV specific-antibodies, were resolved by SDS-PAGE under reducing conditions. Radiolabeled viral proteins are indicated on the right. Lanes: input, virions immediately lysed without cell binding and viral proteins immunoprecipitated with a cocktail of anti-NDV-specific antibodies; + α-NDV, equivalent amount of virions preincubated with neutralizing anti-NDV-specific antibody prior to incubation with cell monolayers; bound, virus bound to cell monolayers. (B) Binding efficiency of particles represented as a percentage of total input radiolabeled HN protein among particles released from untreated cells (black bar) and mβCD-treated cells (gray bar) bound to cell monolayers. Cells were treated with (+) or without (−) mβCD and anti-NDV antibodies (α-NDV). Results are averages of three experiments, and error bars indicate standard deviations. (C) NDV-cell fusion visualized by dequenching of R18 upon fusion of R18-loaded virions with ELL-0 cells. Virus (strain AV [generated from untreated ELL-0 cells]) was incubated with cells at 4°C for 60 min only (panel ii), virus was bound at 4°C for 60 min and then incubated at 37°C for 30 min or 60 min (panels iii and iv, respectively), or virus that had been preincubated with neutralizing anti-NDV antibody was incubated at 4°C for 60 min and then at 37°C for 30 min (panel v). (D) Kinetics of R18 dequenching and fluorescence upon incubation of R18-loaded NDV (strain B1), released from untreated or mβCD-treated cells, with untreated and neuraminidase (NA)-treated target erythrocytes at 37°C. Results are averages of three experiments, and error bars indicate standard deviations. Results with open symbols were identical and overlap. R18 fluorescence is shown in arbitrary (arb.) units.

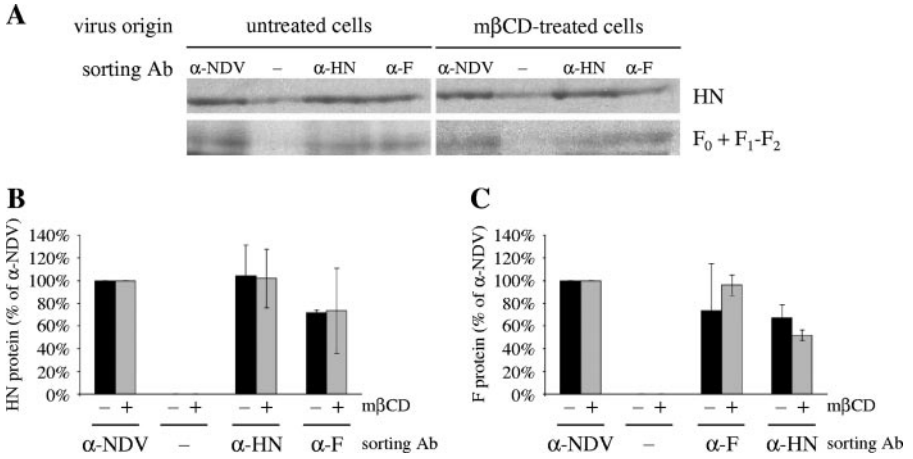

FIG. 3. Precipitation of intact particles with glycoprotein-specific antibodies. Intact ^{35}S-radiolabeled virions released from untreated or mβCD-treated NDV (AV)-infected ELL-0 cells were purified and immunoprecipitated by either polyclonal anti-NDV antibody, HN protein-specific antibody, a mix of F protein-specific antibodies, or no antibody (−) as described in Materials and Methods. Ab, antibody; α-NDV, anti-NDV antibody. (A) A representative autoradiograph of the HN and F protein content of particles released from untreated and mβCD-treated cells precipitated with anti-NDV antibody, no antibody (−), anti-HN protein antibody, or anti-F protein antibodies. The virus particle origin is indicated above the gels, and radiolabeled viral proteins are indicated to the right of the gels. HN protein lanes were from polyacrylamide gels electrophoresed under reducing conditions, while F protein lanes were from polyacrylamide gels electrophoresed under nonreducing conditions. (B) Amounts of radiolabeled HN protein in particles released from untreated cells (black bars) and mβCD-treated cells (gray bars). Particles were precipitated or "sorted" with antibodies as indicated at the bottom of panel and as described in Materials and Methods. Data are represented as percentages of total HN protein precipitated with anti-NDV. The no-antibody (−) values were subtracted from each precipitation. (C) Amounts of radiolabeled $F_0 + F_1 - F_2$ protein in particles released from untreated cells (black bars) and mβCD-treated cells (gray bars). Particles were "sorted" with antibodies as indicated and as described in Materials and Methods. Data are represented as percentages of total $F_0 + F_1 - F_2$ protein precipitated with anti-NDV. The no-antibody (−) values were subtracted from each precipitation. Results are averages of three experiments, and error bars indicate standard deviations.

incubation at 37°C and peaked at 40 to 60 min (Fig. 2D). At 60 min at 37°C, the extent of hemifusion of particles released from untreated cells was approximately threefold higher than that of particles released from mβCD-treated cells (Fig. 2D). Both hemifusion events were specific, as incubation of particles with neuraminidase-treated cells did not result in transfer or dequenching of R18 (Fig. 2D). Thus, particles released from mβCD-treated cells are deficient in virus-cell hemifusion.

Incorporation of HN-F glycoprotein-containing complexes into virions. Reduced virus-cell hemifusion could be due to reduced virion incorporation of F protein or the packaging of nonfunctional F protein into particles. To address the former possibility, virions were "sorted" with mono-specific antibody, and levels of one glycoprotein were quantified following precipitation of intact particles with antibody specific for the other glycoprotein. ^{35}S-radiolabeled virions, released from untreated and mβCD-treated avian cells, were incubated with antibody specific for the HN protein or a cocktail of antibodies specific for the F protein. Total particles were precipitated with anti-NDV antibody, and nonspecific precipitation was monitored by omission of antibody. Representative autoradiographs of proteins in precipitated particles are shown in Fig. 3A along with quantification of HN and F protein levels (Fig. 3B and C, respectively) within antibody-sorted particles.

Specific precipitation of virion HN protein with HN protein-specific antibody resulted in recovery of approximately 100% of HN protein-containing particles released from untreated cells (Fig. 3B), and the majority of HN protein-containing particles released from untreated cells were precipitated with F protein-specific antibodies (Fig. 3B). Very similar results were obtained with virions released from mβCD-treated cells (Fig. 3B), indicating that all particles contained some level of HN protein. Precipitation of particles with anti-HN protein antibody resulted in recovery of virion-associated F protein similar to that recovered after precipitation with anti-F protein antibodies among virions released from either untreated or mβCD-treated cells (Fig. 3C). Taken together, these results suggested that the majority of particles released from mβCD-treated cells possessed both HN and F glycoproteins within the same virus particle.

HN-F protein-containing complexes in virion envelopes. Given that most particles contain at least some of both the HN proteins and F proteins, we next addressed the effects of cellular cholesterol depletion on packaging of HN-F glycoprotein-containing complexes into virions (Fig. 4). Virions released from untreated or mβCD-treated cells were lysed, and the extent of coimmunoprecipitation of the HN and F proteins was quantified. A representative result of HN and F protein coimmunoprecipitation is depicted in Fig. 4A with quantified results shown in Fig. 4B and C. Approximately 40% of the total virion HN protein in particles released from untreated cells was precipitated with F protein-specific antibodies (Fig. 4B), while in the reciprocal immunoprecipitation, 35% of the total F protein was precipitated with HN protein-specific antibodies (Fig. 4C). In contrast, only 20% of the total HN protein in particles released from mβCD-treated cells was precipitated with F protein-specific antibodies (Fig. 4B). In the reciprocal immunoprecipitation, the amount of total F protein precipitated with HN protein-specific antibodies was reduced threefold (Fig. 4C). The significant reduction in virion-associated

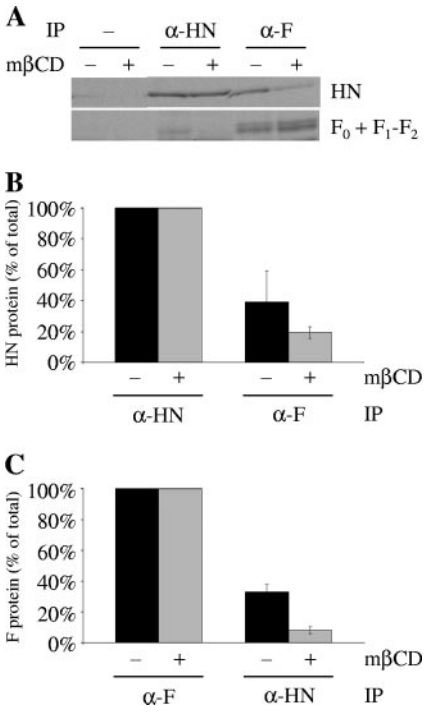

FIG. 4. Coimmunoprecipitation of HN and F proteins from virions released from untreated and mβCD-treated avian cells. Purified ^{35}S-radiolabeled virions released from untreated and mβCD-treated ELL-0 cells were lysed, and proteins were immunoprecipitated (IP) with a mix of anti-HN protein-specific antibodies or a mix of anti-F protein-specific antibodies as outlined in Materials and Methods. α-HN, anti-HN antibodies; α-F, anti-F antibodies. (A) A representative autoradiograph of virions from untreated or mβCD-treated cells precipitated with no antibody (−) or with anti-HN protein or anti-F protein antibodies. Radiolabeled, precipitated viral proteins are indicated on the right. HN protein lanes were from polyacrylamide gels electrophoresed under reducing conditions, while F protein lanes were from polyacrylamide gels electrophoresed under nonreducing conditions. (B) Amounts of radiolabeled HN protein specifically precipitated with anti-HN protein- or anti-F protein-specific antibodies from solubilized virions released from untreated cells (black bars) or mβCD-treated cells (gray bars). Data are represented as percentages of total HN protein precipitated with anti-HN protein-specific antibodies set at 100% for each virus. (C) Amounts of radiolabeled F protein specifically precipitated with anti-F protein- or anti-HN protein-specific antibodies from solubilized virions released from untreated cells (black bars) or mβCD-treated cells (gray bars). Data are represented as percentages of total F protein precipitated with anti-F protein-specific antibodies set at 100% for each virus. Results are averages of three experiments, and error bars indicate standard deviations.

HN-F protein-containing complexes in particles released from cholesterol-depleted cells could account for their reduced infectivity, since F protein activation is thought to require interactions with HN protein.

Cell surface distribution of viral glycoproteins after cholesterol depletion. To explore the mechanisms for reduction in HN and F protein complexes in virions released from mβCD-treated cells, these glycoprotein complexes in infected cells were characterized. First, the effects of cholesterol depletion on the cell surface distribution of HN and F proteins were examined by immunofluorescence microscopy. Both the HN and F glycoproteins (Fig. 5A and B, respectively) formed small, distinct foci across the surfaces of untreated avian cells. However, upon treatment of avian cells with mβCD, there was a dramatic redistribution of both proteins. Several large HN protein-specific patches formed (Fig. 5A). In contrast, F protein redistributed primarily to the cell periphery (Fig. 5B). On the surfaces of infected HEL cells, the HN and F proteins (Fig. 5C and D, respectively) each formed discrete foci. The HN protein on the surfaces of NPC cells localized in distinct foci, but the F protein stained diffusely over the cell surface (Fig. 5C and D, respectively). Qualitatively, the surface localizations of HN and F proteins on infected NPC cells differed from the surface localizations of the glycoproteins on mβCD-treated avian cells. These differences may be due to additional effects that mβCD has on the avian cell cytoskeleton. In any event, loss of plasma membrane cholesterol alters the glycoprotein surface distribution in both types of cells, and this alteration results in the same reduction of virus infectivity when particles are assembled and released from these two cell types. The redistribution of surface glycoproteins when levels of plasma membrane cholesterol were decreased, due either to mβCD treatment or to endogenous cholesterol transport defects, suggested that the viral protein-protein interactions in the plasma membrane may be altered in cells depleted of cholesterol.

Effects of cholesterol depletion on viral glycoprotein complexes in cell extracts. The effects of cholesterol depletion on the detection of HN and F protein complexes in infected avian cells were characterized by quantifying the extent of coimmunoprecipitation of the two proteins as in Fig. 4. A representative coimmunoprecipitation is shown in Fig. 6A with quantifications of multiple experiments shown in Fig. 6B and C. Nearly 75% of the total cell-associated HN protein in untreated cell extracts was precipitated with F protein-specific antibodies (Fig. 6B), while in the reciprocal immunoprecipitation, approximately 70% of the total F protein was precipitated with HN protein-specific antibodies (Fig. 6C). In contrast, only 35% of the total HN protein in mβCD-treated cell extracts was precipitated with F protein-specific antibodies (Fig. 6B). In the reciprocal immunoprecipitation, the amount of F protein precipitated with HN protein-specific antibodies was 20% of the total F protein (Fig. 6C). The significant reduction in coimmunoprecipitation of HN and F proteins after cholesterol depletion strongly indicated that viral protein-protein interactions in the cells were altered when cellular cholesterol levels were depleted.

HN-F glycoprotein complexes in cellular DRM fractions. We have previously reported that NDV assembly occurs in lipid raft domains (18). If the HN and F protein complexes detected in total cellular extracts are assembled into virions, then these complexes should be detected in the cellular DRM fractions previously characterized (18). Indeed, in untreated cell extracts, the HN protein in DRM fractions was precipitated with F protein-specific antibodies, although the majority of HN and F protein complexes were detected in DRM-L fractions (Fig. 7D). Only F protein in DRM-L fractions was precipitated with HN protein-specific antibodies (Fig. 7E). Importantly, there was little significant coimmunoprecipitation of the two proteins from detergent-soluble, nonraft fractions of untreated cells (Fig. 7), indicating that the HN-F protein complexes reside in lipid raft domains.

As previously reported, in mβCD-treated cells, there was a reduced association of HN and F proteins with DRM-L frac-

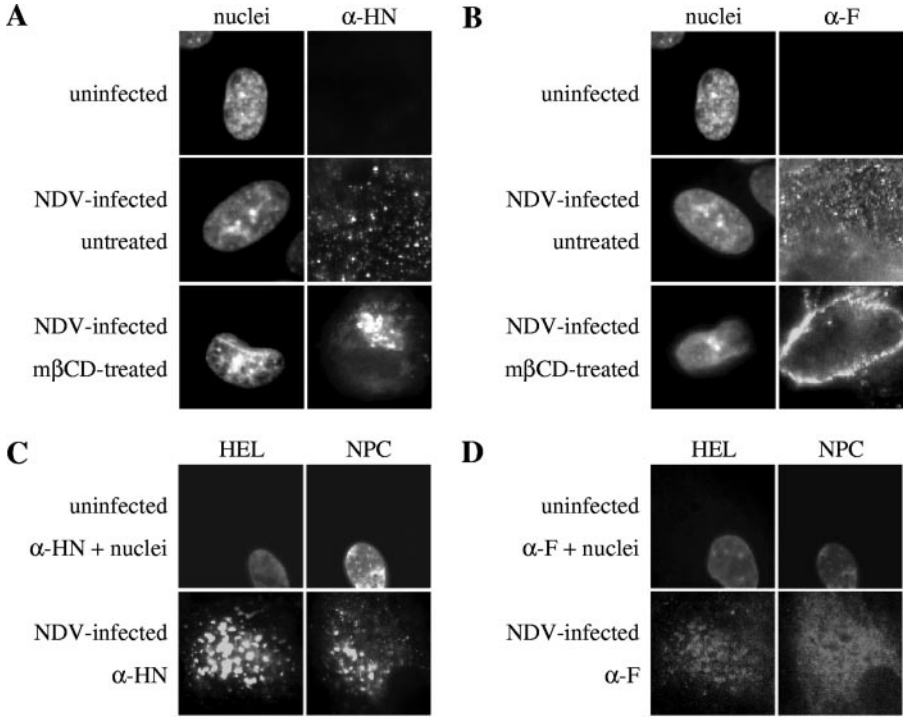

FIG. 5. HN and F glycoprotein surface distribution on untreated and mβCD-treated avian cells, HEL cells, and NPC cells. (A and B) Surface distribution of HN protein (A) or F protein (B) on ELL-0 cells as visualized by fluorescence microscopy. Uninfected cells were left untreated. At 7 h postinfection, NDV (AV)-infected cells were left untreated or treated with 10 mM mβCD and lovastatin for 1 hour, followed by a 1-hour recovery incubation in DMEM. Cells were fixed, incubated with antibodies specific for HN protein or F protein (α-HN or α-F, respectively), and processed for immunofluorescence microscopy as described in Materials and Methods. (C and D) Surface distribution of HN protein (C) or F protein (D) on uninfected and NDV (AV)-infected HEL and NPC cells as visualized by fluorescence microscopy. At 8 h postinfection, cells were fixed, stained for surface HN protein or F protein, and processed for immunofluorescence microscopy as described in Materials and Methods.

tions and an increase of the proteins in detergent-soluble fractions of the cell (18) (Fig. 7B and C, respectively). Most importantly, there was very little coimmunoprecipitation of protein from either the DRM-L or DRM-H fraction or, significantly, from detergent-soluble fractions of mβCD-treated cells (Fig. 7D and E). These results indicate that detection of HN and F protein complexes by coimmunoprecipitation depends upon the presence of cholesterol and membrane raft integrity.

Effects of virion envelope cholesterol depletion. Although extraction of cholesterol from virion membranes had no effect on NDV infectivity (18), the importance of cholesterol in virion membranes for detection of virion-associated HN-F protein-containing complexes and in glycoprotein functions was tested. ^{35}S-radiolabeled virions, generated from untreated avian cells, were depleted of cholesterol by incubation with increasing concentrations of mβCD and then repurified (Fig. 8). Incubation of particles with 10 mM mβCD removed approximately 90% of virion-associated cholesterol as previously reported (18). Approximately 40% of the total HN protein from untreated particles was precipitated with F protein-specific antibody (Fig. 8A), while in the reciprocal coimmunoprecipitation, ~40% of total F protein was precipitated with HN protein-specific antibody (Fig. 8B). Cholesterol extraction of virion membranes had no effect on the precipitation of HN protein with F protein-specific antibody (Fig. 8A). The amount of F protein precipitated with HN protein-specific antibody was not decreased but rather somewhat increased (~55% of the total) (Fig. 8B).

The cell binding efficiency of untreated particles was approximately 20%, and cholesterol extraction had no significant effect on virus binding efficiencies (Fig. 8C). Cholesterol extraction of virions did not inhibit virus-cell membrane fusion as measured in the R18 hemifusion assay described above (Fig. 8D). Indeed, the hemifusion of mβCD-treated particles was increased by cholesterol extraction. These results indicate that extraction of cholesterol from the virion envelope did not affect the association of the HN and F glycoproteins nor was it inhibitory to activities of the two glycoproteins.

DISCUSSION

Results presented here and previously indicate that perturbation of membrane lipid raft domains either by extraction of cholesterol with mβCD or by their aberrant formation in Niemann-Pick syndrome type C fibroblasts resulted in the abnormal assembly and release of relatively noninfectious Newcastle disease virus particles. Particles released from mβCD-treated cells had normal attachment activity but were defective in fusion of viral and cellular membranes. This reduced fusion correlated with a significant reduction in detection of HN-F protein-containing complexes in the virion envelopes of these particles and with loss of HN and F protein-containing complexes in mβCD-treated cells. However, extraction of choles-

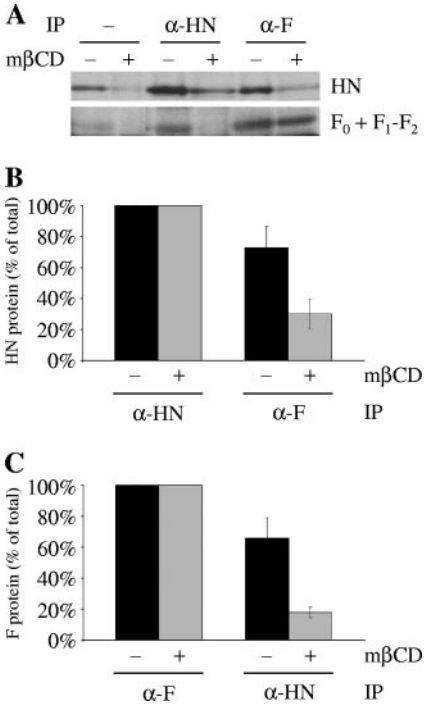

FIG. 6. Coimmunoprecipitation of viral glycoproteins from cellular extracts of untreated and mβCD-treated avian cells. Monolayers of NDV(AV)-infected ELL-0 cells were pulse-labeled with [^{35}S]methionine/cysteine at 6 h postinfection and then subjected to a 1-hour nonradioactive chase. Cells were then left untreated (−) or treated with 10 mM mβCD and lovastatin for 1 hour (+), incubated in DMEM for 1 hour, and then lysed as described in Materials and Methods. Proteins in extracts were immunoprecipitated (IP) with a mix of anti-HN protein-specific antibodies (α-HN) or a mix of anti-F protein-specific antibodies (α-F) as outlined in Materials and Methods. To detect total F ($F_0 + F_1 - F_2$) protein, proteins were electrophoresed in the absence of reducing agent. (A) A representative autoradiograph of cell extracts from untreated or mβCD-treated cells precipitated with no antibody (−) or with anti-HN protein or anti-F protein antibodies. Radiolabeled viral proteins are indicated on the right. (B) Amounts of radiolabeled HN protein specifically precipitated with anti-HN protein- or anti-F protein-specific antibodies from cellular extracts of untreated cells (black bars) or mβCD-treated cells (gray bars). Data are represented as percentages of total HN protein precipitated with anti-HN protein-specific antibodies set at 100% for each cell extract. (C) Amounts of radiolabeled F protein precipitated with anti-F protein- or anti-HN protein-specific antibodies from cellular extracts of untreated cells (black bars) or mβCD-treated cells (gray bars). Data are represented as percentages of total F protein precipitated with anti-F protein-specific antibodies set at 100% for each cell extract. Results are averages of three experiments, and error bars indicate standard deviations.

terol from virion membranes did not affect these preformed HN and F protein complexes. Taken together, these results suggest that membrane lipid rafts facilitate the necessary viral protein-protein interactions for the proper assembly of infectious NDV particles.

Assembly and release of virus from NPC cells. Because mβCD has been shown to not only disrupt membrane lipid rafts but also to affect cytoskeleton organization (17), it was important to characterize assembly and release of particles from cells with membrane lipid rafts disordered by another mechanism. NPC cells are reported to have altered membrane lipid raft domains (9, 10, 22, 39, 44). These cells were derived from humans with a specific lysosomal storage disorder (14). The NPC disease is primarily due to a mutation(s) in the *NPC1* gene, which encodes a protein involved in the transport of low-density-lipoprotein-derived cholesterol (14, 46) and likely endogenously synthesized cholesterol (35) to various organelles, including the plasma membrane. In NPC cells, cholesterol, as well as raft-associated sphingolipids (39), accumulate in late endosomes and lysosomes. The actual level of cholesterol in the plasma membranes of NPC cells is controversial (2, 4, 20, 44), but it is clear that the lipid organization and function of membrane rafts at the plasma membrane of these cells are abnormal (2, 11, 16, 44).

NPC cells and wild-type counterpart (HEL) cells were equally permissive to NDV infection, and both NDV glycoproteins were found at comparable levels on the surfaces of infected HEL and NPC cells. Importantly, the actin cytoskeleton of NPC cells was similar to that observed for the control HEL cells. However, there was reduced association of the viral proteins with DRMs from NPC cells compared to HEL cells, consistent with altered membrane lipid rafts in NPC cells. Similar to previous results with mβCD-treated avian cells (18), particles released from NPC cells were characterized by irregular protein composition and reduced infectivity compared to particles released from control HEL cells. These results suggest that abnormal membrane lipid rafts, due to mutation in cholesterol transport, have effects on the assembly of infectious virus similar to the effects of disruption of membrane lipid rafts by cholesterol extraction with mβCD. The results are consistent with the conclusion that the integrity of membrane lipid rafts is important for the proper assembly and release of infectious virions.

Effects of infected-cell cholesterol depletion on released virions. Disruption of infected-cell lipid raft domains resulted in release of virions with reduced infectivity, and the results shown here suggest that reduced infectivity was not due to loss of virus-cell attachment but may be attributed to defects in virus-cell membrane fusion. The fusion defect may be due to either insufficient levels of F protein incorporation into particles or due to packaging of inactive F proteins. Experiments "sorting" particles with HN protein- or F protein-specific antibodies showed that most virions, whether derived from untreated or mβCD-treated cells, contained both glycoproteins. Furthermore, that all particles contained HN protein was shown by the observation that the cell binding of particles released from untreated and mβCD-treated cells was identical. One limitation to this experimental sorting approach is the inability to determine the relative levels of each glycoprotein packaged into a single particle. It is possible that there are particles with low levels of incorporated HN protein or F protein, which could potentially impact the overall infectivity of the virion population. Nonetheless, most particles released from mβCD-treated cells possessed both HN and F glycoproteins, suggesting that the packaged F proteins may be inactive.

Studies of cell-cell membrane fusion mediated by paramyxovirus glycoproteins have shown that fusion requires activation of the F protein by the homologous viral attachment protein following cell attachment (19). The activated F protein then proceeds through a series of conformational changes that initiate hemifusion, pore formation, and pore expansion (19).

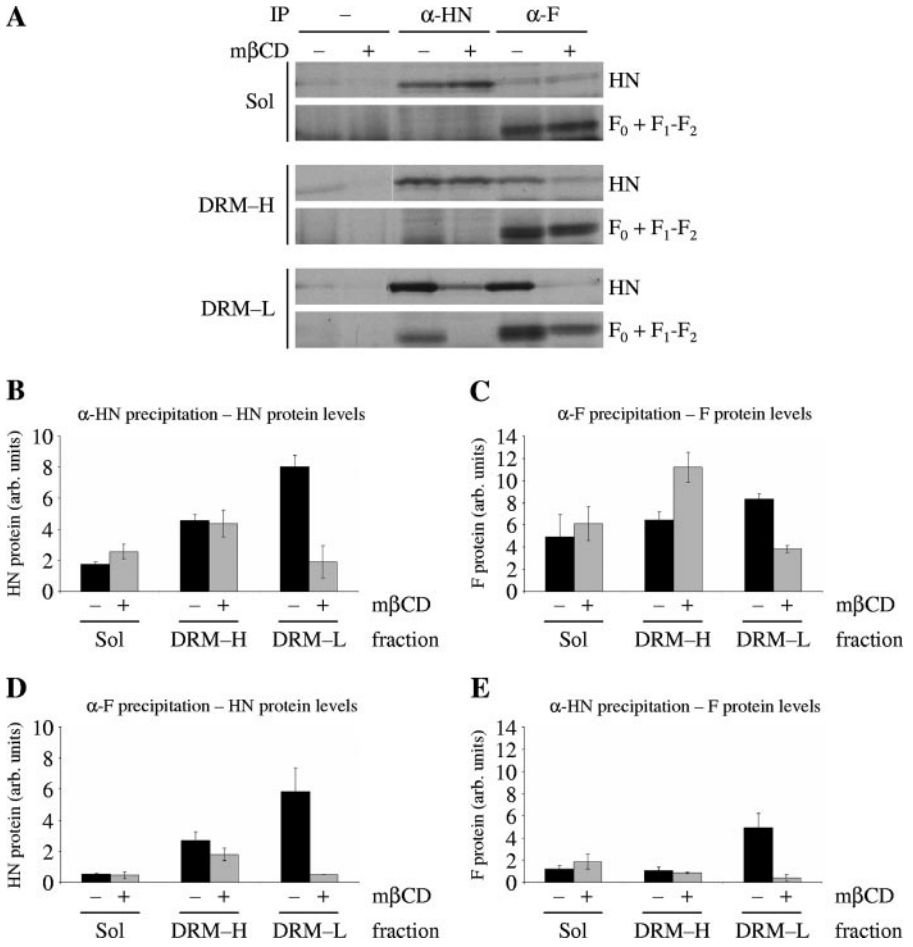

FIG. 7. Immunoprecipitation of viral proteins from DRM cell fractions derived from untreated and mβCD-treated avian cells. Cellular extracts of NDV(AV)-infected ELL-0 cells, untreated (−) or treated with 10 mM mβCD and lovastatin (+), were prepared as described in the legend to Fig. 6 and separated into DRM-L, DRM-H, and detergent-soluble fractions as described in the legend to Fig. 1C. Gradient fractions corresponding to the three cellular fractions as indicated in Fig. 1C were pooled, and proteins were immunoprecipitated (IP) with mono-specific antibodies. (A) A representative autoradiograph of proteins precipitated from gradient fractions (Sol, detergent-soluble gradient fractions; DRM-H, heavy [high-density] DRM gradient fractions; DRM-L, light [low-density] DRM gradient fractions) derived from untreated or mβCD-treated cells precipitated with no antibody (−) or with anti-HN protein- or anti-F protein-specific antibodies. Radiolabeled viral proteins are indicated on the right. (B) Radiolabeled HN protein specifically precipitated with anti-HN protein-specific antibodies from indicated cellular fractions of untreated cells (black bars) or mβCD-treated cells (gray bars). Data are represented as absolute HN protein levels (arbitrary [arb.] densitometer units) precipitated with anti-HN protein-specific antibodies. (C) Radiolabeled F protein specifically precipitated with anti-F protein-specific antibodies from indicated cellular fractions of untreated cells (black bars) or mβCD-treated cells (gray bars). Data are represented as absolute F protein levels (arbitrary densitometer units) precipitated with anti-F protein-specific antibodies. (D) Radiolabeled HN protein specifically precipitated with anti-F protein-specific antibodies from indicated cellular fractions of untreated cells (black bars) or mβCD-treated cells (gray bars). Data are represented as absolute HN protein levels (arbitrary densitometer units) precipitated with anti-F protein-specific antibodies. (E) Radiolabeled F protein specifically precipitated with anti-HN protein-specific antibodies from indicated cellular fractions of untreated cells (black bars) or mβCD-treated cells (gray bars). Data are represented as absolute F protein levels (arbitrary densitometer units) precipitated with anti-HN protein-specific antibodies. Results are averages of three experiments, and error bars indicate standard deviations.

Because virions released from cholesterol-deficient cells were defective in hemifusion, the first step in membrane fusion, it was possible that these virions were defective in F protein activation. Failure to activate the F protein could be due to loss of necessary HN and F protein-containing complexes required for membrane fusion. To test the possibility that virus released from mβCD-treated cells had reduced HN and F protein complexes, the levels of these complexes in particles released from untreated cells were first determined. There have been numerous reports of paramyxovirus attachment protein and fusion protein complexes in infected and transfected cells (1, 5, 21, 34, 42). Indeed, NDV HN and F protein complexes were efficiently detected in transiently transfected HN and F protein-expressing cells (24). However, there has been very little characterization of associations between glycoproteins within paramyxovirus particles. Using conditions previously utilized to detect NDV HN and F protein complexes in cellular extracts of transfected cells (24), HN and F protein complexes were detected in virions. However, while 70% and 60% of total HN and F protein, respectively, in infected-cell extracts were precipitated with heterologous antibody, only 40% of the total virion-associated HN protein and 35% of the total virion-

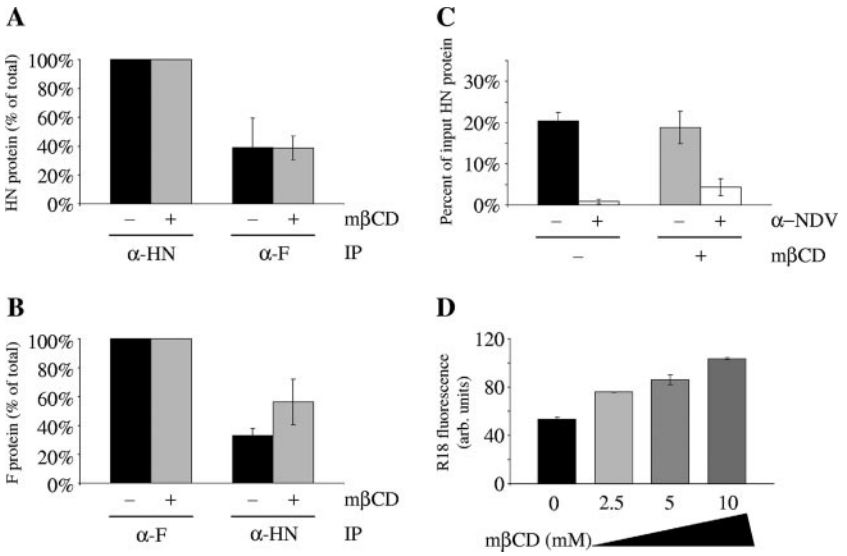

FIG. 8. Effects of cholesterol extraction from virions on viral glycoprotein interactions and activities. ^{35}S-radiolabeled virions released from untreated NDV (AV)-infected ELL-0 cells were left untreated (−) or depleted of cholesterol with 2.5, 5, or 10 mM mβCD (+) for 1 h at 37°C and then repurified as described in Materials and Methods. IP, immunoprecipitate; α- HN, anti-HN antibodies; α-F, anti-F antibodies. (A) Levels of coimmunoprecipitation of HN protein from solubilized particles either untreated (black bars) or treated with 10 mM mβCD (gray bars) as described in the legend to Fig. 4 and in Materials and Methods. Results are averages of three experiments, and error bars indicate standard deviations. (B) Levels of coimmunoprecipitation of F protein from solubilized particles either untreated (black bars) or treated with 10 mM mβCD (gray bars) as described in the legend to Fig. 4 and in Materials and Methods. Results are averages of three experiments, and error bars indicate standard deviations. (C) Virus-cell binding efficiency, measured as described in the legend to Fig. 2, of particles left untreated (black bar) or treated with 10 mM mβCD (gray bar). Inhibition of cell binding by preincubation of virions with anti-NDV antibody is shown in white bars. Results are averages of three experiments, and error bars indicate standard deviations. (D) Extent of virus-cell membrane hemifusion, measured as described in the legend to Fig. 2 and Materials and Methods, for particles left untreated or treated with increasing concentrations of mβCD. The R18 fluorescence (in arbitrary [arb.] units) of target erythrocytes at 1 h at 37°C is shown for each sample. Results are averages of three experiments, and error bars indicate standard deviations.

associated F protein could be precipitated with heterologous antibody. These results suggest that virion-associated glycoproteins are heterogeneous and that packaging of glycoproteins into virions selects individual glycoprotein oligomers along with HN and F protein complexes.

The detection of HN and F protein-containing complexes in the envelopes of particles released from mβCD-treated cells was significantly reduced. As it is well-documented that paramyxovirus cell-cell fusion is dependent on F protein interactions with homologous viral attachment proteins (13), the reduction in hemifusion between particles released from mβCD-treated cells and target cell membranes may be attributed to the reduction of HN and F protein complexes. While it cannot be ruled out that HN and F protein complexes are reduced due to altered ratios of HN and F proteins in individual particles, given the existence of near-normal levels of virion F_1 protein in particles released from mβCD-treated cells (18), it seems more likely that virion-incorporated F protein is nonfunctional due to loss of interactions with virion-incorporated HN protein.

Effects of cholesterol depletion on glycoprotein complexes in infected cells. The reduction of HN and F protein complexes in virus released from mβCD-treated cells and the altered cell surface distribution of the two glycoproteins after cholesterol extraction suggested that membrane lipid raft integrity may have a role in detection of HN and F protein complexes in cell extracts. In fact, cell-associated HN-F protein-containing complexes were detected exclusively in cellular DRM fractions and were not detected in detergent-soluble fractions of cells. Strikingly, cholesterol extraction resulted in significantly reduced detection of glycoprotein complexes in total extracts and in residual DRM domains. Significantly, HN and F protein complexes did not shift to detergent-soluble fractions of mβCD-treated cells, suggesting that the integrity of membrane lipid raft domains is important for the formation or maintenance of these complexes. Preliminary data also demonstrated a significant loss in detection of these complexes specifically from cellular DRM fractions of infected NPC cells (J. Laliberte and T. Morrison, unpublished data).

Recently, Ono et al. described a role for cholesterol in facilitating viral protein-protein interactions at membrane raft domains (31). Depletion of cellular cholesterol by mβCD treatment reduced the ability of human immunodeficiency virus type 1 Gag protein to multimerize and fractionate with DRMs, resulting in impaired virus release (31). These results are consistent with those presented here and suggest that cholesterol and membrane lipid raft integrity is important for viral protein interactions and assembly of infectious virions.

Effects of cholesterol depletion on virion-associated glycoprotein complexes. To address the roles of membrane lipid rafts in the formation and maintenance of glycoprotein complexes, cholesterol was extracted from normal virions. Removal of approximately 90% of virion-associated cholesterol (18) did not affect detection of HN and F protein complexes, indicating that, once formed and incorporated into virions, these complexes were not dependent upon membrane lipid raft

integrity. Supporting this conclusion was the observation that cholesterol extraction of virion envelopes had no effect on particle infectivity (18), virus-cell attachment, or virus-cell hemifusion. Also consistent with this conclusion are results reported by Dolganiuc et al. examining the role of cholesterol in cell-cell fusion by NDV HN and F protein-expressing cells (6). HN and F protein-expressing cells, which were acutely depleted of cholesterol with mβCD, fused R18-loaded target erythrocytes to levels similar to those of HN and F protein-expressing cells left untreated (6). Thus, extraction of cholesterol had no effect on F protein activation and therefore, perhaps, the integrity of these preformed HN and F protein complexes. Together, these results suggest that once formed, HN and F protein complexes in virions, and perhaps in cells, are stable and functional after cholesterol removal. Although the stability of these glycoprotein complexes in cells is under investigation, the results support the hypothesis that formation, and not maintenance, of the NDV HN and F protein complex is cholesterol/membrane lipid raft-dependent. Detection of HN and F protein complexes in the mutant NPC cells is significantly reduced in comparison to the wild-type HEL cells (Laliberte and Morrison, unpublished). This result suggests that proper association of the glycoproteins with normal membrane lipid rafts may be essential for the formation of the glycoprotein complex following biosynthesis. The residual fusion activity and low levels of HN and F protein complexes detected in virus released from mβCD-treated cells could be due to complexes formed during the 2 hours of pulse-chase labeling prior to cholesterol extraction of infected-cell membranes.

In conclusion, the results presented here show that extraction of cholesterol from infected-cell membranes, but not virion envelopes, decreases the infectivity of released virus by hindering the packaging of functional F proteins into virions. Results are consistent with the proposal that cholesterol, and its role in maintaining membrane lipid raft domains in NDV-infected cells, facilitates the formation or maintenance of HN-F protein complexes and, therefore, the virion incorporation of glycoprotein complexes capable of initiating virus-cell membrane fusion.

ACKNOWLEDGMENTS

We thank Mark Peeples (Ohio State University) and Timothy Kowalik (University of Massachusetts Medical School) for anti-Fu1a and monoclonal anti-M antibodies and HEL cells, respectively.

This work was supported by National Institutes of Health AI30572.

REFERENCES

1. **Aguilar, H. C., K. A. Matreyek, C. M. Filone, S. T. Hashimi, E. L. Levroney, O. A. Negrete, A. Bertolotti-Ciarlet, D. Y. Choi, I. McHardy, J. A. Fulcher, S. V. Su, M. C. Wolf, L. Kohatsu, L. G. Baum, and B. Lee.** 2006. N-glycans on Nipah virus fusion protein protect against neutralization but reduce membrane fusion and viral entry. J. Virol. **80:**4878–4889.
2. **Blom, T. S., M. Koivusalo, E. Kuismanen, R. Kostiainen, P. Somerharju, and E. Ikonen.** 2001. Mass spectrometric analysis reveals an increase in plasma membrane polyunsaturated phospholipid species upon cellular cholesterol loading. Biochemistry **40:**14635–14644.
3. **Connolly, S. A., and R. A. Lamb.** 2006. Paramyxovirus fusion: real-time measurement of parainfluenza virus 5 virus-cell fusion. Virology **355:**203–212.
4. **Dahl, N. K., K. L. Reed, M. A. Daunais, J. R. Faust, and L. Liscum.** 1992. Isolation and characterization of Chinese hamster ovary cells defective in the intracellular metabolism of low density lipoprotein-derived cholesterol. J. Biol. Chem. **267:**4889–4896.
5. **Deng, R., Z. Wang, P. J. Mahon, M. Marinello, A. Mirza, and R. M. Iorio.** 1999. Mutations in the Newcastle disease virus hemagglutinin-neuraminidase protein that interfere with its ability to interact with the homologous F protein in the promotion of fusion. Virology **253:**43–54.
6. **Dolganiuc, V., L. McGinnes, E. J. Luna, and T. G. Morrison.** 2003. Role of the cytoplasmic domain of the Newcastle disease virus fusion protein in association with lipid rafts. J. Virol. **77:**12968–12979.
7. **Faaberg, K. S., and M. E. Peeples.** 1988. Strain variation and nuclear association of Newcastle disease virus matrix protein. J. Virol. **62:**586–593.
8. **Fenton, R. G., H. F. Kung, D. L. Longo, and M. R. Smith.** 1992. Regulation of intracellular actin polymerization by prenylated cellular proteins. J. Cell Biol. **117:**347–356.
9. **Garver, W. S., R. P. Erickson, J. M. Wilson, T. L. Colton, G. S. Hossain, M. A. Kozloski, and R. A. Heidenreich.** 1997. Altered expression of caveolin-1 and increased cholesterol in detergent insoluble membrane fractions from liver in mice with Niemann-Pick disease type C. Biochim. Biophys. Acta **1361:**272–280.
10. **Garver, W. S., S. C. Hsu, R. P. Erickson, W. L. Greer, D. M. Byers, and R. A. Heidenreich.** 1997. Increased expression of caveolin-1 in heterozygous Niemann-Pick type II human fibroblasts. Biochem. Biophys. Res. Commun. **236:**189–193.
11. **Henderson, L. P., L. Lin, A. Prasad, C. A. Paul, T. Y. Chang, and R. A. Maue.** 2000. Embryonic striatal neurons from Niemann-Pick type C mice exhibit defects in cholesterol metabolism and neurotrophin responsiveness. J. Biol. Chem. **275:**20179–20187.
12. **Hoekstra, D., and K. Klappe.** 1986. Use of a fluorescence assay to monitor the kinetics of fusion between erythrocyte ghosts, as induced by Sendai virus. Biosci. Rep. **6:**953–960.
13. **Hu, X. L., R. Ray, and R. W. Compans.** 1992. Functional interactions between the fusion protein and hemagglutinin-neuraminidase of human parainfluenza viruses. J. Virol. **66:**1528–1534.
14. **Ikonen, E., and M. Holtta-Vuori.** 2004. Cellular pathology of Niemann-Pick type C disease. Semin. Cell Dev. Biol. **15:**445–454.
15. **Kilsdonk, E. P., P. G. Yancey, G. W. Stoudt, F. W. Bangerter, W. J. Johnson, M. C. Phillips, and G. H. Rothblat.** 1995. Cellular cholesterol efflux mediated by cyclodextrins. J. Biol. Chem. **270:**17250–17256.
16. **Koike, T., G. Ishida, M. Taniguchi, K. Higaki, Y. Ayaki, M. Saito, Y. Sakakihara, M. Iwamori, and K. Ohno.** 1998. Decreased membrane fluidity and unsaturated fatty acids in Niemann-Pick disease type C fibroblasts. Biochim. Biophys. Acta **1406:**327–335.
17. **Kwik, J., S. Boyle, D. Fooksman, L. Margolis, M. P. Sheetz, and M. Edidin.** 2003. Membrane cholesterol, lateral mobility, and the phosphatidylinositol 4,5-bisphosphate-dependent organization of cell actin. Proc. Natl. Acad. Sci. USA **100:**13964–13969.
18. **Laliberte, J. P., L. W. McGinnes, M. E. Peeples, and T. G. Morrison.** 2006. Integrity of membrane lipid rafts is necessary for the ordered assembly and release of infectious Newcastle disease virus particles. J. Virol. **80:**10652–10662.
19. **Lamb, R. A., and D. Kolakofsky.** 2001. Paramyxoviridae: the viruses and their replication. *In* D. M. Knipe and P. M. Howley (ed.), Fields virology. Lippincott Williams & Wilkins, Philadelphia, PA.
20. **Lange, Y., J. Ye, M. Rigney, and T. Steck.** 2000. Cholesterol movement in Niemann-Pick type C cells and in cells treated with amphiphiles. J. Biol. Chem. **275:**17468–17475.
21. **Li, J., E. Quinlan, A. Mirza, and R. M. Iorio.** 2004. Mutated form of the Newcastle disease virus hemagglutinin-neuraminidase interacts with the homologous fusion protein despite deficiencies in both receptor recognition and fusion promotion. J. Virol. **78:**5299–5310.
22. **Lusa, S., T. S. Blom, E. L. Eskelinen, E. Kuismanen, J. E. Mansson, K. Simons, and E. Ikonen.** 2001. Depletion of rafts in late endocytic membranes is controlled by NPC1-dependent recycling of cholesterol to the plasma membrane. J. Cell Sci. **114:**1893–1900.
23. **McGinnes, L. W., K. Gravel, and T. G. Morrison.** 2002. Newcastle disease virus HN protein alters the conformation of the F protein at cell surfaces. J. Virol. **76:**12622–12633.
24. **McGinnes, L. W., and T. G. Morrison.** 2006. Inhibition of receptor binding stabilizes Newcastle disease virus HN and F protein-containing complexes. J. Virol. **80:**2894–2903.
25. **McGinnes, L. W., and T. G. Morrison.** 1994. The role of the individual cysteine residues in the formation of the mature, antigenic HN protein of Newcastle disease virus. Virology **200:**470–483.
26. **McGinnes, L. W., H. Pantua, and T. G. Morrison.** 2006. Newcastle disease virus: propagation, quantification, and storage, p. 15F.2.1–15F.2.18. *In* R. Coico, T. Kowalik, J. Quarles, B. Stevenson, and R. Taylor (ed.), Current protocols in microbiology. John Wiley & Sons, Inc., Hoboken, NJ.
27. **McGinnes, L. W., J. N. Reitter, K. Gravel, and T. G. Morrison.** 2003. Evidence for mixed membrane topology of the Newcastle disease virus fusion protein. J. Virol. **77:**1951–1963.
28. **Morrison, T. G.** 2003. Structure and function of a paramyxovirus fusion protein. Biochim. Biophys. Acta **1614:**73–84.
29. **Morrison, T. G., M. E. Peeples, and L. W. McGinnes.** 1987. Conformational change in a viral glycoprotein during maturation due to disulfide bond disruption. Proc. Natl. Acad. Sci. USA **84:**1020–1024.

30. **Ono, A., and E. O. Freed.** 2005. Role of lipid rafts in virus replication. Adv. Virus Res. **64:**311–358.
31. **Ono, A., A. A. Waheed, and E. O. Freed.** 2007. Depletion of cellular cholesterol inhibits membrane binding and higher-order multimerization of human immunodeficiency virus type 1 Gag. Virology **360:**27–35.
32. **Pantua, H., L. W. McGinnes, J. Leszyk, and T. G. Morrison.** 2005. Characterization of an alternate form of Newcastle disease virus fusion protein. J. Virol. **79:**11660–11670.
33. **Pickl, W. F., F. X. Pimentel-Muinos, and B. Seed.** 2001. Lipid rafts and pseudotyping. J. Virol. **75:**7175–7183.
34. **Plemper, R. K., A. L. Hammond, D. Gerlier, A. K. Fielding, and R. Cattaneo.** 2002. Strength of envelope protein interaction modulates cytopathicity of measles virus. J. Virol. **76:**5051–5061.
35. **Reid, P. C., S. Sugii, and T. Y. Chang.** 2003. Trafficking defects in endogenously synthesized cholesterol in fibroblasts, macrophages, hepatocytes, and glial cells from Niemann-Pick type C1 mice. J. Lipid Res. **44:**1010–1019.
36. **San Roman, K., E. Villar, and I. Munoz-Barroso.** 2002. Mode of action of two inhibitory peptides from heptad repeat domains of the fusion protein of Newcastle disease virus. Int. J. Biochem. Cell Biol. **34:**1207–1220.
37. **Scheiffele, P., M. G. Roth, and K. Simons.** 1997. Interaction of influenza virus haemagglutinin with sphingolipid-cholesterol membrane domains via its transmembrane domain. EMBO J. **16:**5501–5508.
38. **Sergel, T., L. W. McGinnes, M. E. Peeples, and T. G. Morrison.** 1993. The attachment function of the Newcastle disease virus hemagglutinin-neuraminidase protein can be separated from fusion promotion by mutation. Virology **193:**717–726.
39. **Simons, K., and J. Gruenberg.** 2000. Jamming the endosomal system: lipid rafts and lysosomal storage diseases. Trends Cell Biol. **10:**459–462.
40. **Simons, K., and D. Toomre.** 2000. Lipid rafts and signal transduction. Nat. Rev. Mol. Cell Biol. **1:**31–39.
41. **Sprong, H., P. van der Sluijs, and G. van Meer.** 2001. How proteins move lipids and lipids move proteins. Nat. Rev. Mol. Cell Biol. **2:**504–513.
42. **Stone-Hulslander, J., and T. G. Morrison.** 1997. Detection of an interaction between the HN and F proteins in Newcastle disease virus-infected cells. J. Virol. **71:**6287–6295.
43. **Suomalainen, M.** 2002. Lipid rafts and assembly of enveloped viruses. Traffic **3:**705–709.
44. **Vainio, S., I. Bykov, M. Hermansson, E. Jokitalo, P. Somerharju, and E. Ikonen.** 2005. Defective insulin receptor activation and altered lipid rafts in Niemann-Pick type C disease hepatocytes. Biochem. J. **391:**465–472.
45. **Wang, C., G. Raghu, T. Morrison, and M. E. Peeples.** 1992. Intracellular processing of the paramyxovirus F protein: critical role of the predicted amphipathic alpha helix adjacent to the fusion domain. J. Virol. **66:**4161–4169.
46. **Wojtanik, K. M., and L. Liscum.** 2003. The transport of low density lipoprotein-derived cholesterol to the plasma membrane is defective in NPC1 cells. J. Biol. Chem. **278:**14850–14856.